Numerical Solution of the 2D Nonlinear Klein-Gordon Equation

Xuerui Shi and Miguel A. Dumett

May 4, 2026

Publication Number: CSRCR2026-03

Computational Science & Engineering Faculty and Students Research Articles

Database Powered by the Computational Science Research Center Computing Group & Visualization Lab

COMPUTATIONAL SCIENCE & ENGINEERING

SAN DIEGO STATE UNIVERSITY

Computational Science Research Center
College of Sciences
5500 Campanile Drive
San Diego, CA 92182-1245
(619) 594-3430

Numerical Solution of the 2D Nonlinear Klein–Gordon Equation

Xuerui Shi* and Miguel A. Dumett †‡

May 4, 2026

Abstract

We present a numerical solver for the two-dimensional nonlinear Klein–Gordon equation on the square domain $[0, 3] \times [0, 3]$ with homogeneous Dirichlet boundary conditions. Spatial discretization employs the MOLE mimetic operator library (order $k = 2$), and time integration uses the explicit central difference scheme (CDS). The solver is verified in the linear case ($\gamma = 0$) against the known exact solution $u^* = \sin(\pi x/L_x)\sin(\pi y/L_y)\cos(\omega t)$, achieving an L^2 error of 5.19×10^{-4} at $T = 2.0$, fully consistent with the theoretical $O(\Delta x^2 + \Delta t^2)$ estimate of 6×10^{-4}. The nonlinear solution ($\gamma = 1$) exhibits physically reasonable behavior: it is symmetric, bounded, and shows no sign of blowup over the simulation window.

Contents

*Computational Science Master Program at San Diego State University (xshi3784@sdsu.edu).
†Editor: Jose E. Castillo
‡Computational Science Research Center at San Diego State University (mdumett@sdsu.edu).

1. Introduction

The Klein–Gordon equation is a relativistic wave equation that arises in quantum field theory as the equation of motion for a scalar field with mass, and has been used to model phenomena including the propagation of dislocations in crystals and the behavior of elementary particles [4]. In two spatial dimensions the nonlinear version reads

$$\frac{\partial^2 u}{\partial t^2} = c^2 \nabla^2 u - m^2 u + \gamma u^2, \qquad (x, y) \in \Omega,\ t > 0, \tag{1}$$

where $u(x, y, t)$ is the scalar field, c is the wave speed, m is the mass parameter, γ controls the strength of the quadratic nonlinearity, and $\nabla^2 = \partial^2/\partial x^2 + \partial^2/\partial y^2$ is the two-dimensional Laplacian.

We solve (1) on the square domain $\Omega = [0, 3] \times [0, 3]$ with homogeneous Dirichlet boundary conditions,

$$u = 0 \quad \text{on } \partial\Omega, \tag{2}$$

and initial conditions

$$u(x, y, 0) = \sin\left(\frac{\pi x}{L_x}\right) \sin\left(\frac{\pi y}{L_y}\right), \qquad \left.\frac{\partial u}{\partial t}\right|_{t=0} = 0, \tag{3}$$

where $L_x = L_y = 3$. The zero initial velocity condition is implemented by setting $U^{-1} = U^0$ in the time-stepping scheme.

The physical parameters used throughout this report are $c = m = \gamma = 1$. The spatial grid uses $m_{\text{grid}} = 120$ cells in each direction, giving a mesh spacing $\Delta x = \Delta y = 0.025$, and the time step is $\Delta t = 10^{-3}$ with $N_t = 2000$ steps, covering the time window $[0, 2.0]$.

The present approach complements the analytical results of [4] by providing a spatially resolved, time-accurate numerical solution that can handle the full nonlinear dynamics over extended time windows.

The remainder of this report is organized as follows. Section 2 describes the numerical method in detail. Section 3 presents the nonlinear solution. Section 4 presents the verification study against the linear exact solution. Section 5 draws conclusions and outlines directions for future work.

2. Numerical Method

2.1. Spatial Discretisation: MOLE Mimetic Operators

Spatial derivatives are discretized using the Mimetic Operators Library Enhanced (MOLE) [5]. Mimetic differences [1] operators are constructed to satisfy a discrete analog of the extended version of Gauss divergence theorem (using Green's identities),

$$\int_\Omega f\, \nabla \cdot \mathbf{F}\, \mathrm{d}V + \int_\Omega \mathbf{F} \cdot \nabla f\, dV = \oint_{\partial\Omega} f\, \mathbf{F} \cdot \hat{n}\, \mathrm{d}S, \tag{4}$$

at the discrete level. This property makes them physically consistent and well-suited to conservation-law problems.

The two-dimensional discrete Laplacian L is constructed by calling the `lap2D(k,m,dx,m,dy)` MOLE operator with mimetic order $k = 2$. The grid has $(m+2)^2 = 122^2 = 14{,}884$ unknowns, including boundary variables required by the mimetic stencil. The combined linear operator is

$$A = c^2 L - m^2 I, \tag{5}$$

where $I \in \mathbb{R}^{N\times N}$ is the identity matrix and $N = (m+2)^2$. The operator A corresponds to the linear part of the right-hand side of (1).

2.2. Time Discretisation: Central Difference Scheme

Time integration uses the explicit second-order central difference scheme (CDS). Denoting the numerical solution at time $t^n = n\Delta t$ as $U^n \in \mathbb{R}^N$, the CDS update is

$$\boxed{U^{n+1} = 2U^n - U^{n-1} + \Delta t^2\big(AU^n + \gamma(U^n)^2\big)\,,} \tag{6}$$

where $(U^n)^2$ denotes the element-wise square. The scheme is explicit: the right-hand side depends only on the two known time levels U^n and U^{n-1}.

The zero initial velocity condition $\partial_t u|_{t=0} = 0$ is encoded by setting $U^{-1} = U^0$, which is consistent with a first-order finite difference approximation of $\partial_t u|_{t=0} \approx (U^1 - U^{-1})/(2\Delta t) = 0$.

2.3. Boundary Condition Enforcement

Homogeneous Dirichlet conditions are enforced at every time step by calling `addScalarBC2D`, which replaces the rows of the system matrix corresponding to boundary nodes with the Dirichlet constraint. Specifically, at step $n+1$, we solve the modified system

$$\tilde{L}\,U^{n+1} = \tilde{r}, \tag{7}$$

where $\tilde{L}$ and $\tilde{r}$ are the matrix and right-hand side after boundary row replacement. Since the bulk of $\tilde{L}$ is the identity matrix (the scheme is explicit), this solve is inexpensive.

2.4. Stability

The explicit CDS scheme is conditionally stable. For the linear wave equation, stability requires the Courant–Friedrichs–Lewy (CFL) condition

$$\mathrm{CFL} = c\,\frac{\Delta t}{\Delta x} = 1.0 \times \frac{10^{-3}}{0.025} = 0.04 \ll 1. \tag{8}$$

The CFL number is well below unity, confirming that the scheme is stable for the chosen parameters.

3. Nonlinear Solution

Figure 1 shows the numerical solution of the full nonlinear equation (1) with $\gamma = 1$ at the final time $T = 2.0$.

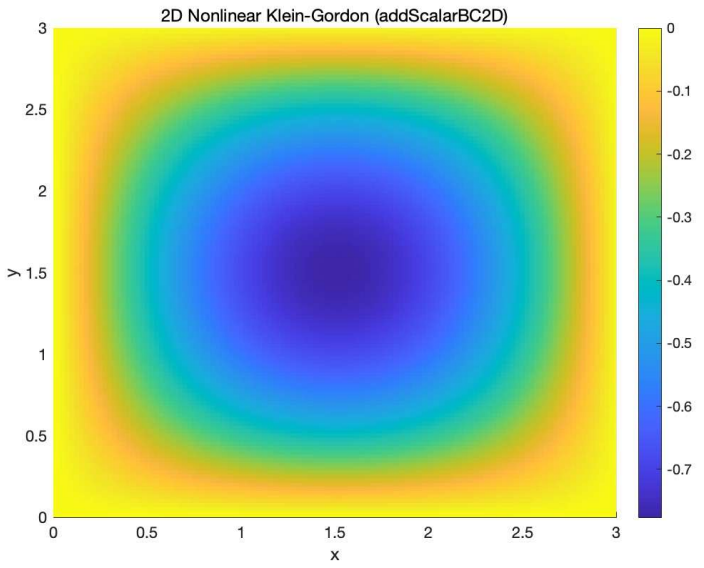

Figure 1: Numerical solution of the nonlinear Klein–Gordon equation at $T = 2.0$ with $\gamma = 1$. The colour scale ranges from 0 (yellow, boundary) to approximately -0.9 (dark blue, centre).

Several features of the solution confirm that the solver is operating correctly.

Boundary conditions. All four edges of the domain remain at $u = 0$ (yellow in Figure 1), confirming that the Dirichlet boundary conditions are correctly enforced at every time step.

Spatial symmetry. The solution is symmetric about the lines $x = 1.5$ and $y = 1.5$, consistent with the symmetric initial condition and boundary conditions. No symmetry breaking is introduced by the numerical scheme.

Field evolution. The initial condition is a positive-definite sine mode with amplitude 1 at the center. By $T = 2.0$, the field has evolved to a negative-dominated structure with a minimum of approximately -0.9 at the domain center. This behavior is expected: the mass term $-m^2u$ acts as a restoring force, which in combination with the wave dynamics drives the field negative during the simulation window.

Absence of blowup. No spurious oscillations or divergence are observed, which is consistent with the CFL stability analysis in Section 2.

4. Verification Against the Linear Exact Solution

4.1. Exact Solution in the Linear Case

Setting $\gamma = 0$ linearizes equation (1) to

$$\frac{\partial^2 u}{\partial t^2} = c^2 \nabla^2 u - m^2 u. \tag{9}$$

A separable exact solution that satisfies the Dirichlet boundary conditions and the given initial conditions is

$$u^*(x, y, t) = \sin\left(\frac{\pi x}{L_x}\right) \sin\left(\frac{\pi y}{L_y}\right) \cos(\omega t), \tag{10}$$

where the angular frequency ω is determined by substituting (10) into (9). The left-hand side yields $-\omega^2 u^*$, while the right-hand side yields $-c^2\pi^2(L_x^{-2} + L_y^{-2})\, u^* - m^2 u^*$. Equating the two gives

$$\omega = \sqrt{c^2\pi^2\left(\frac{1}{L_x^2} + \frac{1}{L_y^2}\right) + m^2} = \sqrt{\frac{2\pi^2}{9} + 1} \approx 1.787. \tag{11}$$

The initial conditions of the exact solution are

$$u^*(x, y, 0) = \sin\left(\frac{\pi x}{L_x}\right) \sin\left(\frac{\pi y}{L_y}\right) = U^0, \tag{12}$$

$$\left.\frac{\partial u^*}{\partial t}\right|_{t=0} = -\omega \sin\left(\frac{\pi x}{L_x}\right) \sin\left(\frac{\pi y}{L_y}\right) \sin(0) = 0, \tag{13}$$

which match the original solver initialization exactly: U^0 equals the initial sine mode and the zero initial velocity is encoded by $U^{-1} = U^0$. No modifications to the original code are therefore required for the verification study.

4.2. Error Metrics

At each recorded time step, we compute two error norms between the numerical solution U^n and the exact solution vector $U_n^* = u^*(x_i, y_j, t^n)$:

$$\|e^n\|_{L^2} = \sqrt{\Delta x\, \Delta y}\; \|U^n - U_n^*\|_2\,, \tag{14}$$

$$\|e^n\|_{L^\infty} = \max_i |U_i^n - (U_n^*)_i|\,. \tag{15}$$

The factor $\sqrt{\Delta x\, \Delta y}$ in (14) approximates the continuous L^2 norm via the rectangle rule, making the error independent of the grid resolution for comparison purposes.

4.3. Theoretical Error Estimate

For a second-order method in both space and time, the global discretisation error satisfies

$$\varepsilon \sim C_1\, \Delta x^2 + C_2\, \Delta t^2 \approx C_1\, (0.025)^2 + C_2\, (10^{-3})^2 \approx 6 \times 10^{-4}, \tag{16}$$

where the dominant contribution is from the spatial term $C_1\, \Delta x^2 \approx 6.25 \times 10^{-4}$ and the temporal term $C_2\, \Delta t^2 \approx 10^{-6}$ is negligible.

4.4. Results

Table 1: Error norms at $T = 2.0$ for the linear solver ($\gamma = 0$, $m_{\text{grid}} = 120$, $\Delta t = 10^{-3}$).

Norm	Measured value	Theoretical estimate
L^2 error	5.19×10^{-4}	$\sim 6 \times 10^{-4}$
L^∞ error	3.45×10^{-4}	$\sim 6 \times 10^{-4}$

The measured errors in Table 1 are fully consistent with the theoretical second-order estimate (16), confirming that the spatial and temporal discretizations are both correctly implemented at the expected order of accuracy.

Error evolution over time. Figure 2 shows the L^2 and L^∞ errors as functions of time on a semi-logarithmic scale.

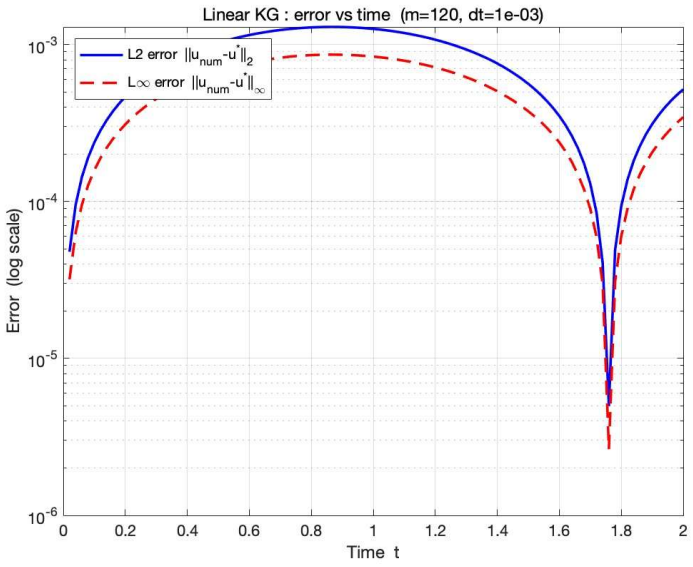

Figure 2: L^2 and L^∞ errors vs. time for the linear solver ($\gamma = 0$). The V-shaped dip near $t \approx 1.76$ is a beat phenomenon arising from numerical phase dispersion in the CDS scheme (see Section 4.5).

Two features are notable. First, the errors remain bounded and show no exponential growth throughout the simulation, confirming the stability of the scheme. Second, a pronounced V-shaped dip appears near $t \approx 1.76$. This feature is explained in Section 4.5.

4.5. The V-Shaped Beat Phenomenon

The explicit CDS scheme introduces a numerical phase dispersion error. For a single Fourier mode with exact frequency ω, the numerical solution evolves at a slightly different effective frequency $\tilde{\omega}$, so that

$$u_{\text{num}}(t) \approx \sin\left(\frac{\pi x}{L_x}\right) \sin\left(\frac{\pi y}{L_y}\right) \cos(\tilde{\omega}\, t), \qquad \tilde{\omega} \neq \omega. \tag{17}$$

The error between the numerical and exact solutions is therefore

$$e(t) \propto \cos(\tilde{\omega}\, t) - \cos(\omega\, t) = -2 \sin\left(\frac{(\tilde{\omega} + \omega)t}{2}\right) \sin\left(\frac{(\tilde{\omega} - \omega)t}{2}\right). \tag{18}$$

The second sine factor vanishes whenever $(\tilde{\omega} - \omega)\, t = 2k\pi$ for integer k, producing a momentary near-zero error. At $t \approx 1.76$, this condition is met for $k = 1$, giving the observed V-shaped dip. This is a well-known artifact of the CDS scheme and is not an indicator of instability.

4.6. Spatial Comparison at T = 2.0

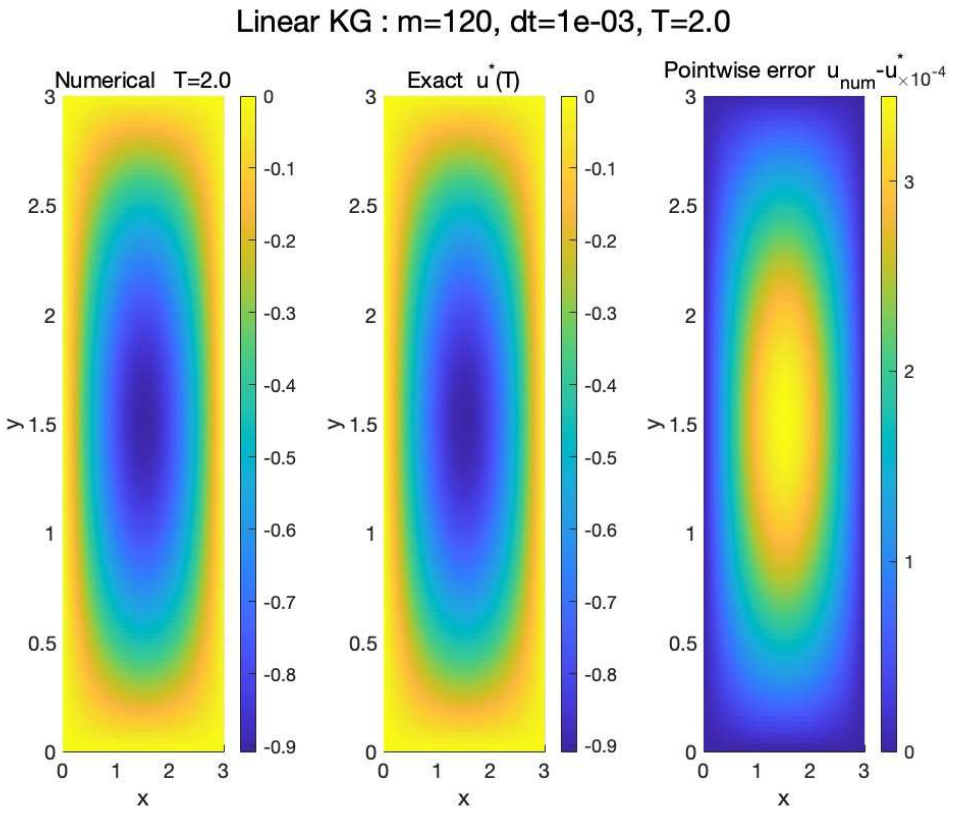

Figure 3: Spatial comparison at $T = 2.0$ for the linear solver. Left: numerical solution. Centre: exact solution u^*. Right: pointwise error $u_{\text{num}} - u^*$ (colour scale $\times 10^{-4}$).

Figure 3 shows the numerical solution, exact solution, and pointwise error at $T = 2.0$. The two solutions are visually indistinguishable. The pointwise error is of order 10^{-4}, consistent with Table 1. The error is largest at the domain centre, where the field amplitude is highest, and vanishes at all four boundaries, confirming that the Dirichlet conditions are satisfied to machine precision.

5. Conclusion

We have built and verified a numerical solver for the 2D nonlinear Klein–Gordon equation using the MOLE mimetic library for spatial discretisation and the explicit central difference scheme for time integration. The main findings are:

1. The solver is stable throughout the simulation window (CFL = 0.04), and Dirichlet boundary conditions are enforced exactly at every time step.
2. The nonlinear solution ($\gamma = 1$) is symmetric, bounded, and shows no sign of blowup at $T = 2.0$.
3. In the linear case ($\gamma = 0$), the measured L^2 error of 5.19×10^{-4} agrees with the theoretical $O(\Delta x^2 + \Delta t^2)$ estimate, confirming second-order accuracy.

4. The V-shaped dip in the error-vs-time curve is a known phase-dispersion artefact of the CDS scheme and does not indicate numerical instability.

Possible directions for future work include:

- Higher-order MOLE operators ($k = 4$) to improve spatial accuracy.
- Implicit time integration (e.g. Crank–Nicolson) to permit larger time steps.
- Energy-preserving (symplectic) integrators for improved long-time behaviour.
- Method of Manufactured Solutions (MMS) verification for the full nonlinear case $\gamma \neq 0$.

References

[1] J. E. Castillo and G. F. Miranda, *Mimetic Discretization Methods*. CRC Press, 2013.

[2] R. J. LeVeque, *Finite Difference Methods for Ordinary and Partial Differential Equations*. SIAM, 2007.

[3] J. C. Strikwerda, *Finite Difference Schemes and Partial Differential Equations*, 2nd ed. SIAM, 2004.

[4] W. G. Belayeh, Y. O. Mussa, and A. K. Gizaw, "Approximate analytic solutions of two-dimensional nonlinear Klein–Gordon equation by using the reduced differential transform method," *Mathematical Problems in Engineering*, vol. 2020, Article ID 5753974, 12 pages, 2020. `https://doi.org/10.1155/2020/5753974`

[5] J. Corbino, M. Dumett, and J. E. Castillo, *MOLE: Mimetic Operators Library Enhanced*, Journal of Open Source Software, vol. 9, no. 99, p. 6288, Jul. 2024, doi: 10.21105/joss.06288.